

## CHAPTER 2

# The Shell Model

### 2.1 Introduction and General Considerations

In the last chapter we considered the bulk properties of the nucleus, that is, we discussed (static or dynamic) properties for which at least a good fraction of all the nucleons in a nucleus participate. In this chapter we are going to talk about a completely different aspect of the nucleus. Indeed, many nuclear properties seem to be describable in terms of the idea that the nucleons in a nucleus are to be considered as independent particles moving on almost unperturbed single particle orbits. The reasons for this, as we stated at the beginning of the first chapter, is the fact that, mostly due to the action of the Pauli and uncertainty principles, the nucleus is not a very dense system. It is now quite well established that the nucleon-nucleon force has an almost infinitely repulsive core (see [Vi 78]) at a radius  $c$  of about  $c=0.4$  fm. Therefore, the ratio of the closest packed volume  $V_c$  to the actual volume  $V$  of a nucleus is [BM 69, Sec. 2.5]

$$\frac{V_c}{V} = \left( \frac{c}{2r_0} \right)^3 \approx \frac{1}{100}.$$

Thus the known “strong” character of the nucleon-nucleon forces is considerably reduced by the fact that the nucleons are, on the average, quite far apart, and therefore “feel” only the tail of the attractive part of the nuclear force. In other words, the violent interactions due to the singular force occur only quite seldom and the system can be described, at least in a first approximation, in terms of independent particle motion. The

fact that despite these considerations the nucleus develops a very well-defined surface, contrary to a gas, is due to a very subtle interplay of the nuclear forces and the Pauli principle [BP 77a]. For a further, more elaborate discussion of these considerations, see also [BM 69, Sec. 2.5]. The mean free path of the nucleons in a nucleus, as can be estimated from scattering experiments, seems to be at least of the order of the dimension of the nucleus [BM 69, Sec. 2.1; KK 68] and is mentioned as the first piece of experimental evidence for the unperturbed particle motion in a nucleus.

The idea of independent particles accepted, it is quite natural to envisage that this single particle motion is governed by some average potential created by all the nucleons in the nucleus. Of course, the motion of the nucleons will be considerably different in the interior of the nucleus, where it is more or less force free, from the one at the surface where the Pauli principle ceases to act and the particles feel a force confining them to the interior of the nucleus.

In this chapter we will briefly describe further experimental evidence for, and the phenomenological description and consequences of, such an average potential.

## 2.2 Experimental Evidence for Shell Effects

If the validity of an average potential in which the nucleons can move independently can be assumed, this immediately has some obvious consequences similar to those with which we are familiar from atomic physics.

The occurrence of the so-called magic numbers 2, 8, 20, 28, 50, 82, and 126 has, from the experimental point of view, been one of the strongest motivations for the formulation of a nuclear shell model. At these proton or neutron numbers, effects analogous to shell closure of electron shells in atoms are observed. Here we will mention just a few of them.

The single-particle separation energy is defined as the energy required to remove the least bound particle from the nucleus. In Fig. 2.1 the observed separation energies for protons and neutrons are shown.

For most nuclei the separation energy is about 8 MeV, although there are quite prominent exceptions at the magic numbers. The separation energy is largest for doubly magic nuclei. Similar exceptions for the separation energy are found for the electrons in noble gases.

The magic numbers can be seen in Fig. 2.2, which shows that the magic and doubly magic nuclei are exceptionally strongly bound. Strong binding means that the nucleus is very stable against excitations, and in Fig. 1.7 we have already shown the variation of the first  $2^+$  state in nuclei as a function of nucleon number. We can see especially pronounced shell effects at the magic numbers, the excitation energy rising sharply in the neighborhood of shell closures. Other collective excitations show the same variation. These examples should be sufficient as a demonstration of the occurrence of magic numbers in nuclei and of the shells corresponding to

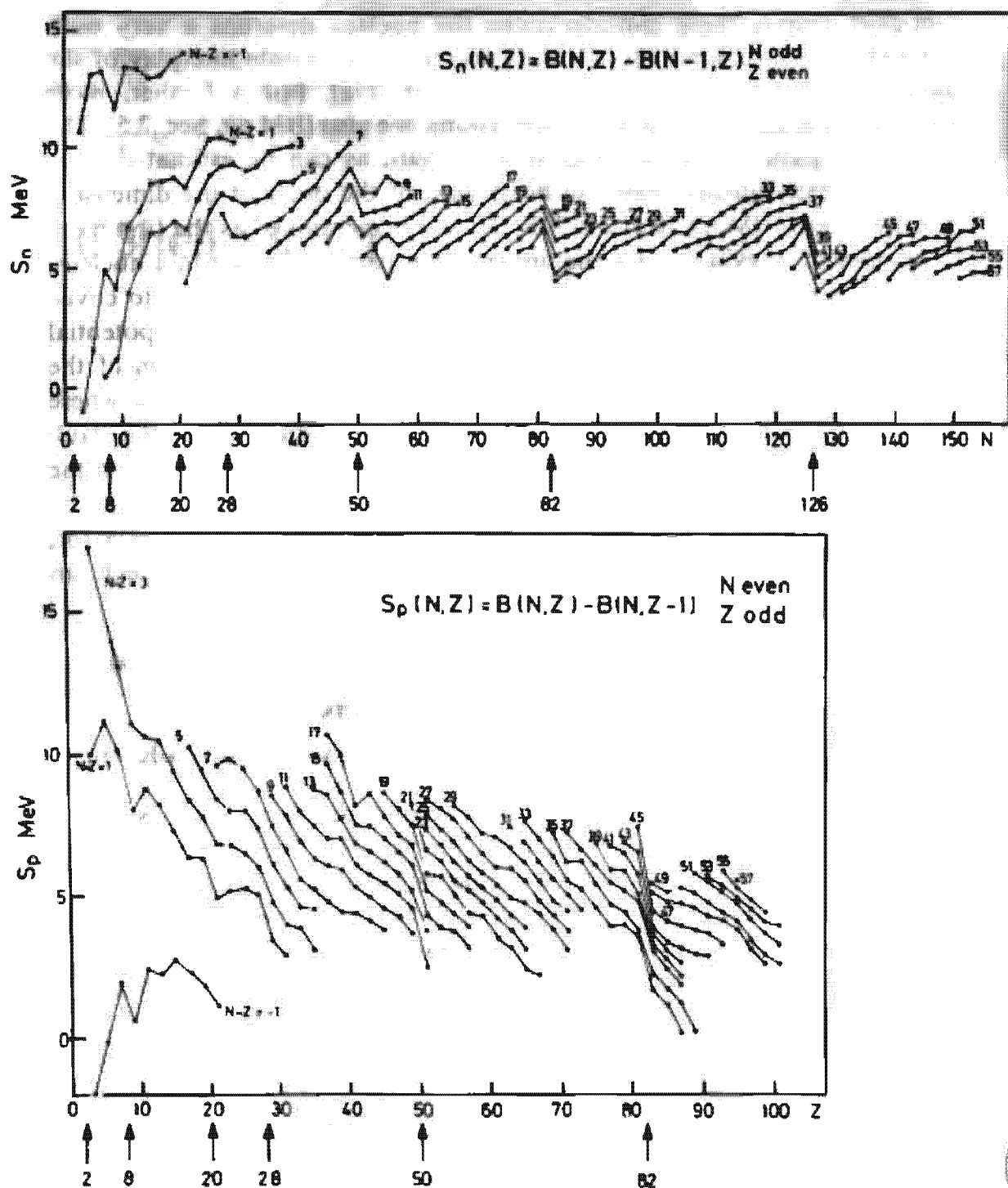


Figure 2.1. Neutron and proton separation energies as a function of neutron and proton number, respectively. (From [Ir 72].)

an average potential analogous to the ones observed in atoms. (More details may be found in [MJ 55].)

### 2.3 The Average Potential of the Nucleus

As mentioned above, the exceptional role of the magic numbers reveals a strong analogy to the situation of the electrons in an atom. There the strong central Coulomb potential of the nucleus imposes sphericity. As a consequence, there exist groups of degenerate levels with quite large energy differences in between the electron shells.

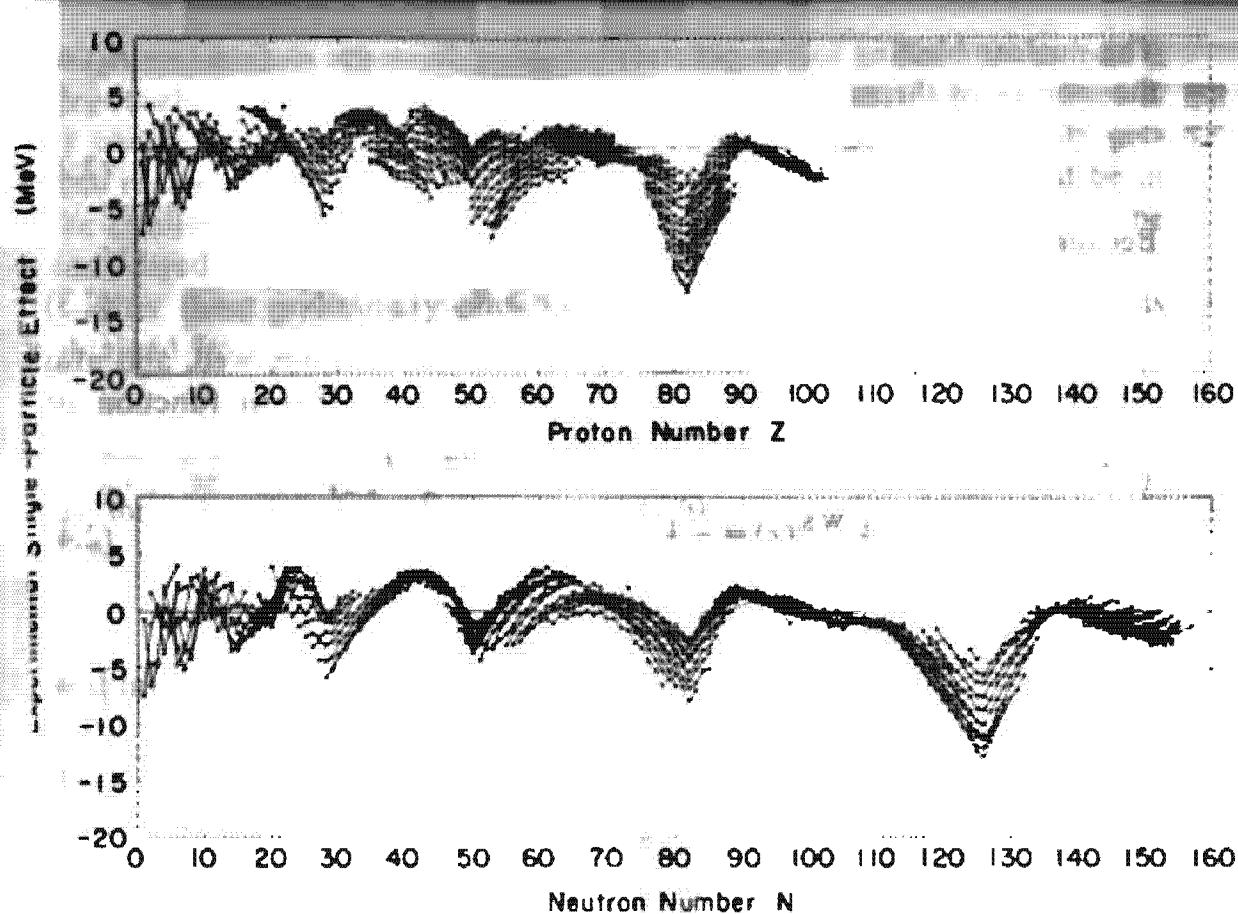


Figure 2.2. Deviations of nuclear masses from their mean values plotted as a function of neutron and proton number. (From [MS 66].)

For the nucleons of a nucleus, there exists a priori no such central field. As we have already discussed in the introduction, however, we can imagine such a potential as being built up by the action of all the nucleons. (Such an average potential also exists in the case of the electrons in an atom; there it makes an extra contribution and has to be added to the nuclear Coulomb potential. The whole is then well known as the Hartree or Hartree-Fock potential of the atom.) A model which describes the dynamics of the nucleons only with such an average potential treats the nucleons as completely independent of one another (the nucleon-nucleon interaction nevertheless comes into it in an indirect way, since it gives rise to the average potential in the first place). In the following, we will call such a model the shell model or independent particle model.

In Chapter 5 we will discuss, in great detail, how one can derive the form of this average field from a microscopic two-body force. In this chapter, we will assume that we have such a one-body potential which describes, to a good approximation, the effects of the mutual interaction between the nucleons, and investigate their consequences.

For further consideration, we have to discuss first the shape of the ad hoc introduced shell model potential. A nucleon close to the center of the nucleus will feel the nuclear forces uniformly, that is, there will be no net force

$$\left( \frac{\partial V(r)}{\partial r} \right)_{r=0} = 0. \quad (2.1)$$

The nuclear binding forces get stronger going from the surface ( $r = R_0$ ) to the interior of the nucleus:

$$\left(\frac{\partial V}{\partial r}\right)_{r < R_0} > 0. \quad (2.2)$$

Because of the finite range of the nuclear forces, we have:

$$V(r) \approx 0, \quad r > R_0. \quad (2.3)$$

An analytic ansatz which represents these conditions quite well, and also yields quite reasonable density distributions, is the Fermi function or *Woods-Saxon potential* [WS 54] (Fig. 2.3):

$$V^{WS}(r) = -V_0 \left[ 1 + \exp\left(\frac{r - R_0}{a}\right) \right]^{-1} \quad (2.4)$$

with

$$R_0 = r_0 A^{1/3}; \quad V_0 \approx 50 \text{ [MeV]}; \quad a \approx 0.5 \text{ [fm]}; \quad r_0 \approx 1.2 \text{ [fm]}.$$

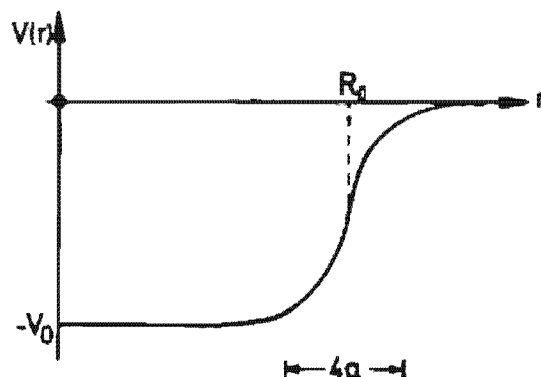


Figure 2.3. Shape of the Woods-Saxon potential.

(The Woods-Saxon potential actually has a finite but negligible slope at  $r = 0$ .) Since the eigenfunctions for this potential cannot be given in closed form, one often uses the following two approximations for qualitative considerations, and also for calculations:

(i) harmonic oscillator

$$V(r) = -V_0 \left[ 1 - \left( \frac{r}{R_0} \right)^2 \right] = \frac{m}{2} \omega_0^2 (r^2 - R_0^2) \quad (2.5)$$

(ii) square well

$$V(r) = \begin{cases} -V_0 & \text{for } r \leq R_0, \\ +\infty & \text{for } r > R_0. \end{cases} \quad (2.6)$$

Before we discuss the solutions of Eqs. (2.4), (2.5), and (2.6) in more detail, we should perhaps note that all three potentials are spherically symmetric. For the moment, we will restrict our considerations to this case; the discussion of deformed potentials will be taken up in Section 2.8. Furthermore, it should be pointed out that (2.5) and (2.6) represent somewhat unphysical potentials, since they are infinite. However as long as we are

only interested in bound single-particle states, this is not too serious a drawback, as only the exponential tails of the wave functions are affected. If one considers excitations in these potentials, however, one easily gets into regions in which the states in the realistic potential (2.4) would be in the continuum. The use of infinite potentials in such cases is then to be considered with extreme care.

After these preliminary remarks, we want to discuss the energy levels obtained from the solution of the eigenvalue problem

$$\left\{ -\frac{\hbar^2}{2m}\Delta + V(r) \right\} \phi_i(r) = \epsilon_i \phi_i(r) \quad (2.7)$$

for the case of the potentials (2.5) and (2.6).

As is well known, the harmonic oscillator gives equidistant energy levels

$$\epsilon_N = \hbar\omega_0 \left( N + \frac{3}{2} \right) - V_0 \quad (2.8)$$

with

$$N = 2(n-1) + l, \quad \text{where } n = 1, 2, \dots, \text{ and } l = 0, 1, 2, \dots \quad (2.9)$$

These levels are  $D(N)$ -fold degenerate:

$$D(N) = \frac{1}{2}(N+1)(N+2), \quad (2.10)$$

where  $N$  is the number of quanta in the oscillator,  $n$  is the radial quantum number,  $l$  is the angular momentum, and  $\omega_0$  is the oscillator frequency. The oscillator constant  $\omega_0$  is usually determined from the mean square radius of a sphere

$$\langle R^2 \rangle = \frac{1}{A} \sum_{i=1}^A \langle r^2 \rangle_i \approx \frac{3}{5} (1.2A^{1/3})^2 [\text{fm}^2]. \quad (2.11)$$

For oscillator states we can calculate  $\langle r^2 \rangle_i$  and get

$$\frac{m}{2} \omega_0^2 \langle r^2 \rangle_i = \frac{\hbar\omega_0}{2} \left( N_i + \frac{3}{2} \right).$$

Together with Eq. (2.10), we find [Mo 57, p. 469]

$$\hbar\omega_0 \approx \frac{5}{4} \left( \frac{3}{2} \right)^{1/3} \frac{\hbar^2}{mr_0^2} A^{-1/3} = 41 \cdot A^{-1/3} [\text{MeV}] \quad (2.12)$$

and for the oscillator length

$$b = \sqrt{\frac{\hbar}{m\omega_0}} = 1.010 \cdot A^{1/6} [\text{fm}]. \quad (2.13)$$

The levels with a definite  $N$  we call an oscillator shell. Because of Eq. (2.9), the oscillator shells only contain either even or odd  $l$ -values, that is one oscillator shell contains only states with the same parity. It also follows from (2.9) that levels with the same  $N$  and with different  $n$  and  $l$  are degenerate. This accidental degeneracy of the harmonic oscillator is removed in the square-well potential (Fig. 2.4). The true energies lie between the two limits given by the potentials of Eqs. (2.5) and (2.6).

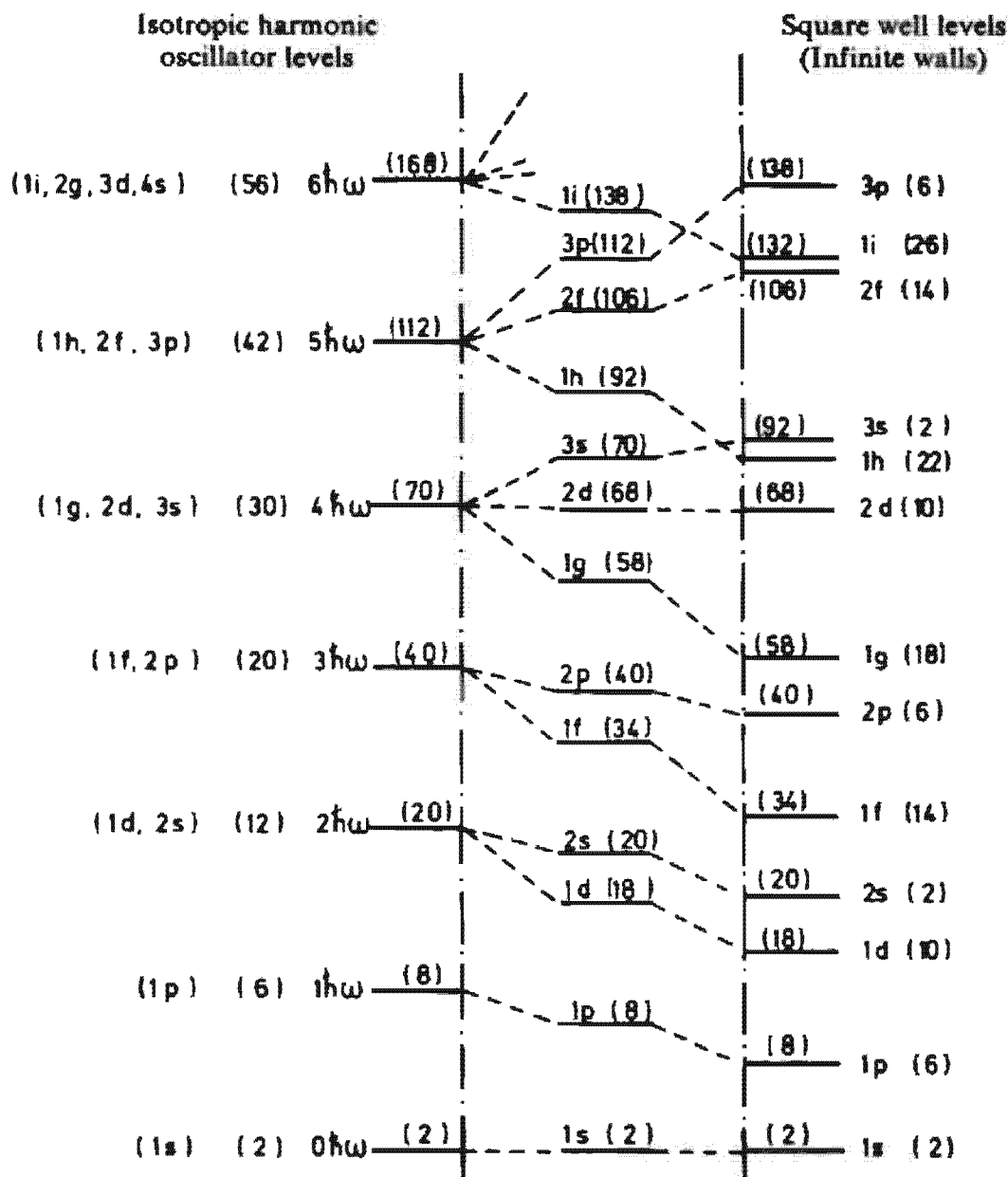


Figure 2.4. Level scheme of the isotropic harmonic oscillator (l.h.s.) and of the infinite square well (r.h.s.). (From [MJ 55]).

Filling up the level scheme with nucleons (by analogy with the periodic system of the atoms), we see that according to the Pauli principle,  $D(N)$  protons and  $D(N)$  neutrons can be put into each oscillator shell. This means that both potentials reproduce the magic numbers 2, 8, and 20. This model can therefore account for the unusual stability of  ${}^4\text{He}_2$ ,  ${}^{16}\text{O}_8$ , and  ${}^{40}\text{Ca}_{20}$ . On the other hand, Fig. 2.4 contains no indications for the higher magic numbers. We will see in the next section how this deficiency of this simple model can be removed. Later, we will also discuss how the Coulomb interaction of the protons influences the average potential (Sec. 2.5).

## 2.4 Spin Orbit Coupling

Up to now, we have not taken into account the spin of the nucleons (apart from a factor of 2 in determining the magic numbers), that is, we considered the nuclear forces as spin independent. Treating the electrons in

atoms relativistically yields a spin dependent force in the form of a spin orbit coupling

$$f(r)\mathbf{l}\cdot\mathbf{s}. \quad (2.14)$$

This gives a splitting of the otherwise degenerate levels with  $j = l \pm \frac{1}{2}$ . In the nucleus such a splitting has also been found experimentally. Scattering of protons or neutrons on  $\alpha$  particles yields for the lowest resonance the (unbound) ground state of  ${}^5\text{Li}$  or  ${}^5\text{He}$ . According to Fig. 2.4 these lowest resonances should have the quantum numbers  $l = 1$ ,  $j = \frac{1}{2}, \frac{3}{2}$ , as the  $1s$ -shell in  ${}^4\text{He}$  is closed. One observes resonances at 1.25 and 2.4 MeV for the scattering of neutrons and protons, respectively. At these energies the angular distributions show that the resonances are predominantly  $j = \frac{3}{2}$ , whereas the  $j = \frac{1}{2}$  resonances lie a few MeV higher in energy.

It was a decisive idea (Haxel, Jensen, and Suess [HJS 49]; Goeppert-Mayer [Ma 49]) to incorporate a strong spin orbit term into the single-particle Hamilton operator of Eq. (2.7). It was only then that the success of the shell model was confirmed. Mathematically this yields a  $jj$ -coupling scheme, since  $\mathbf{l} \cdot \mathbf{s}$  commutes with  $s^2, l^2, j^2, j_z$  but not with  $l_z$  and  $s_z$ . The levels are characterized in this coupling scheme by the quantum numbers  $n, l, j$  (e.g.,  $(2d_{\frac{3}{2}}) \hat{=} (n=2, l=2, j=2+\frac{1}{2})$ ), and a single particle wave function takes the following form\*:

$$\phi(\mathbf{r})_{nsljm} = \langle \mathbf{r} | nsljm \rangle = \phi_{nl}(r) \sum_{m_l m_s} C_{\frac{1}{2} m_s}^{l m_l j m} Y_{lm}(\theta, \phi) | \frac{1}{2} m_s \rangle. \quad (2.15)$$

With the relations

$$\begin{aligned} 2\mathbf{l}\cdot\mathbf{s} |sljm\rangle &= (j^2 - l^2 - s^2) |sljm\rangle \\ &= [j(j+1) - l(l+1) - \frac{3}{4}] |sljm\rangle \end{aligned} \quad (2.16)$$

we are able to give the spin orbit splitting of the doubly degenerate levels  $|slj = l \pm \frac{1}{2}\rangle$  for  $f(r) = \text{const.}$ :

$$\Delta E(l) \sim [l - (-l-1)] = 2l+1. \quad (2.17)$$

An attractive spin orbit potential will assure the experimentally observed fact that the  $l + \frac{1}{2}$  levels are energetically always below the  $l - \frac{1}{2}$  levels. Equation (2.17) shows furthermore that the splitting increases with growing values of  $l$ .

Inclusion of the spin orbit interaction to the interpolated level scheme of Fig. 2.4 yields the modified level scheme of Fig. 2.5. The model now reproduces all magic numbers correctly. The sequence of the levels within the different shells depends on the choice of  $f(r)$ .

The value of  $f(r)$  which one could derive by analogy with the theory of electrons in an atom using a Lorentz invariant treatment of the electromagnetic interactions of the nucleons (Thomas term: cf. [MJ 55, p. 60] and [EG 70, Chap. 8]) turns out to be about an order of magnitude too small.

\* For calculations one has to pay particular attention to the coupling order of the angular momenta, since a different order introduces a phase which is the source of frequent errors.



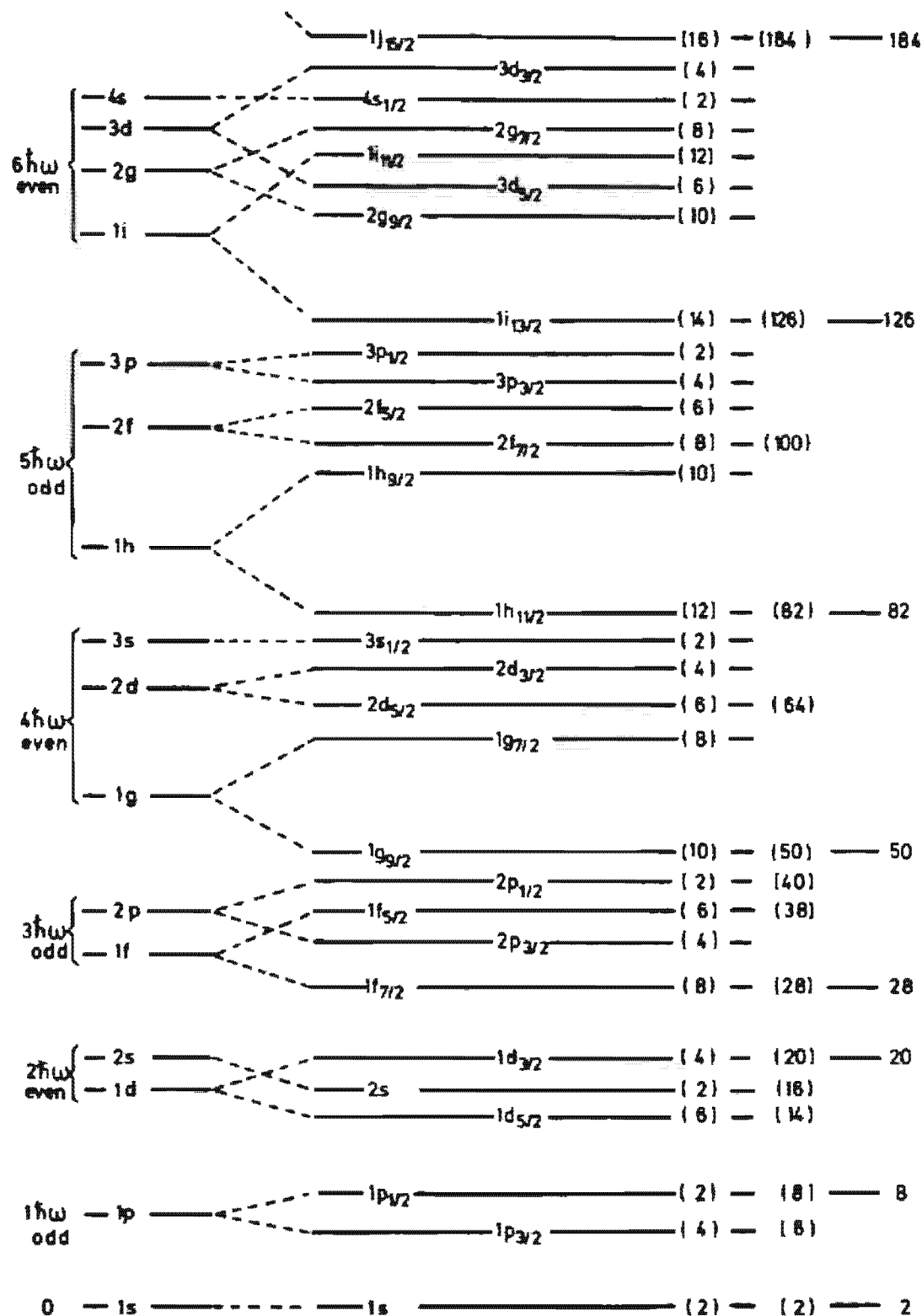


Figure 2.5. Schematic nuclear levels of the shell model with spin orbit term. (From [MJ 55].)

As we will discuss in Chapter 4, the nucleon-nucleon forces exhibit strong spin orbit parts, and it is thus not very surprising that the average single particle potential also has a spin orbit part with a strength compatible with the strong nuclear forces.\*

\*Recent investigations have shown that one obtains the proper spin orbit term in the single-particle potential by a relativistic Hartree-Fock treatment of one-boson-exchange-potentials [Br 78].

One can show [Ho 75] that  $f(r)$  is peaked at the nuclear surface. By analogy with the electronic case, one quite often chooses  $f(r)$  related to the spin independent part of the average potential in the following way—

$$f(r) = \lambda \frac{1}{r} \frac{dV}{dr}; \quad \lambda \simeq -0.5 \text{ [fm}^2\text{]} \quad (2.18)$$

—but also other surface-peaked radial dependences of  $f(r)$  can be envisaged. It is interesting to note that the use of the Skyrme force (see Chap. 5) yields a spin orbit dependence for the average potential with  $f(r) \sim (1/r) \cdot (d\rho/dr)$ , where  $\rho$  is the single particle density. Since  $V(r)$  roughly follows the form of  $\rho$ , this is consistent with Eq. (2.18).

## 2.5 The Shell Model Approach to the Many-Body Problem

The single-particle model takes into account the individual nucleons. It therefore provides a microscopic description of the nucleus. This is certainly only an approximation of the exact many-body problem. We will see, however, in the following, that the shell model can be used as a basis for more elaborate many-body theories, so before we talk about further details of the model, we want to discuss some general properties of the single particle model.

The microscopic theory of the nucleus is usually based on the following three properties.

- (i) The nucleus is a quantum mechanical many-body system.
- (ii) The velocities in the nucleus are small enough so that one can neglect relativistic effects  $[(v/c)^2 \sim 1/10]$ .
- (iii) The interaction between the nucleons has a two-body character.

A full microscopic theory of the nucleus would then be given by the solution of the many-body Schrödinger equation

$$H\Psi = \left\{ \sum_{i=1}^A -\frac{\hbar^2}{2m} \Delta_i + \sum_{i<j}^A v(i, j) \right\} \Psi(1, \dots, A) = E\Psi(1, \dots, A), \quad (2.19)$$

where  $i$  represents all coordinates of the  $i$ th nucleon, for instance,

$$(i) = (r_i, s_i, t_i), \quad (2.20)$$

where  $t_i$  will be  $\frac{1}{2}$  for neutrons and  $-\frac{1}{2}$  for protons. With the assumption of the nuclear shell model, the above equation reduces to the much simpler equation

$$H_0\Psi = \left\{ \sum_{i=1}^A h_i \right\} \Psi = \sum_{i=1}^A \left\{ -\frac{\hbar^2}{2m} \Delta_i + V(i) \right\} \Psi = E\Psi. \quad (2.21)$$

The solutions  $\Psi$  of Eq. (2.21) are anti-symmetrized products of single-particle functions, which are eigenfunctions to the single-particle Hamilto-

nian  $h_i$ :

$$h_i \phi_k(i) = \epsilon_k \phi_k(i). \quad (2.22)$$

The functions  $\phi_k$  provide an orthogonal basis for an occupation number representation within the framework of second quantization (see Appendix C). To each level  $k$  corresponds a pair of creation and annihilation operators  $a_k^+$ ,  $a_k$  which create or annihilate particles with wave function  $\phi_k$ . Since nucleons are Fermions, each level can be occupied only once, and the operators  $a_k$ ,  $a_k^+$  obey Fermi commutation relations (C. 23).

The shell model Hamiltonian  $H_0$  has the form

$$H_0 = \sum \epsilon_k a_k^+ a_k.$$

Using the bare vacuum  $|-\rangle$  its eigenfunctions can be represented as

$$|\Phi_{k_1 \dots k_A}\rangle = a_{k_1}^+ \dots a_{k_A}^+ |-\rangle.$$

They are Slater determinants

$$\Phi_{k_1 \dots k_A}(1, \dots, A) = \begin{vmatrix} \phi_{k_1}(1) & \dots & \phi_{k_1}(A) \\ \vdots & & \vdots \\ \phi_{k_A}(1) & & \phi_{k_A}(A) \end{vmatrix} \quad (2.23)$$

with eigenvalues

$$E_{k_1 \dots k_A} = \epsilon_{k_1} + \dots + \epsilon_{k_A}. \quad (2.24)$$

In the ground state the levels are filled successively according to their energy (see Fig. 2.6)

$$|\Phi_0\rangle = a_1^+ \dots a_A^+ |-\rangle. \quad (2.25)$$

Thus we have for closed shells the following unique prescription for the construction of the  $A$  particle ground state as well as for the  $A$  particle excitation spectrum: Starting with the  $(1s_{1/2})$  level, one has to occupy each level  $|nsljm\rangle$  with just one particle until all  $A$  particles are used up. We thus obtain an  $A$  nucleon ground state where all different quantum states are occupied with just one particle up to the Fermi level (the highest occupied level); above the Fermi level all levels are unoccupied.

The independent particle picture of the nucleus is different from that in an atom in the sense that in a nucleus there are *two* different kinds of particles, the proton and the neutron, whereas in an atom there is only the

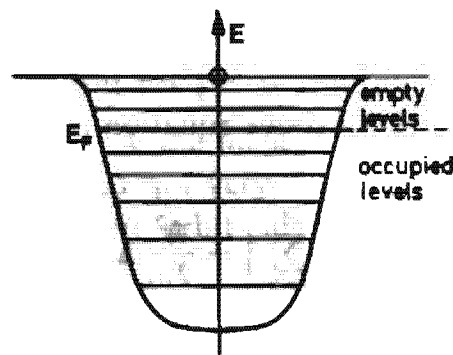


Figure 2.6. Shell model potential and Fermi level.

electron. Protons and neutrons feel different average potentials for two reasons:

- (i) Protons also interact via the *Coulomb force*. One therefore usually adds the potential of a homogeneously charged sphere

$$V_C(r) = \begin{cases} \frac{Ze^2}{R} \frac{1}{2} \left( 3 - \left( \frac{r}{R} \right)^2 \right) & r \leq R, \\ \frac{Ze^2}{r} & r > R. \end{cases} \quad (2.26)$$

Sometimes (see Sec. 2.8), this feature is approximated by using different potential parameters for protons and neutrons.

- (ii) The *symmetry energy* [see Eq. (1.4)] favors a configuration with an equal number of protons and neutrons. Because of the Coulomb repulsion for heavier nuclei, one has a neutron excess: If, in the nucleus, we replace a neutron by a proton, we gain symmetry energy and lose Coulomb energy. Since the Coulomb energy is already taken into account by Eq. (2.26), there must be an additional difference between the single-particle potential for protons and neutrons, which is caused by the symmetry energy. The *nuclear* part of the proton potential is therefore deeper (see Fig. 2.7, dashed line).

These two effects go in opposite directions, but they do not cancel. In the end, the Fermi surfaces for protons and neutrons must be equal, otherwise protons would turn into neutrons by  $\beta$ -decay or vice versa, whichever is energetically favored.

In  $N \neq Z$  nuclei, energy levels with the same quantum numbers for protons and neutrons are therefore shifted with respect to one another by an amount  $\Delta_\epsilon$  resulting from a positive contribution  $\Delta_C$  from the Coulomb force and a negative contribution  $-\Delta_S$  from the symmetry energy

$$\epsilon_{nlf}^{(p)} - \epsilon_{nlf}^{(n)} = \Delta_\epsilon = \Delta_C - \Delta_S. \quad (2.27)$$

In heavy nuclei, this difference is such that the protons and neutrons at the Fermi surface belong to different major shells.

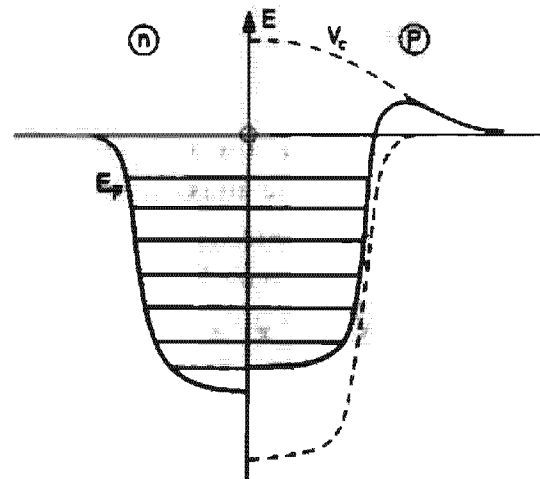


**Figure 2.7.** Comparison of the shell model potential for neutrons and protons in a nucleus with neutron excess.

Strong support of the independent particle idea comes from the experimental fact that magic numbers are the same for protons and neutrons (see Fig. 2.2; the magic number 126 exists only for neutrons, since for the heaviest nucleus known so far we only have  $Z=103$ ). If correlations played a major role, then, for example, the neutron excess in heavier nuclei would eventually influence the proton magic numbers in these nuclei (the nuclear force is almost charge independent; see Chap. 4) to be different from the corresponding neutron numbers. However, as we have said, this is not the case. The subshells of a major shell have, in some cases, a different order.

In the shell model, the *excitations of the system* are given by analogy with the free Fermi gas by a transfer of nucleons from below the Fermi level to levels above it. In the case of only a single nucleon transfer, we talk of an  $1p-1h$  state with excitation energy of  $\sim \hbar\omega_0$ . For  ${}^{40}_{20}\text{Ca}_{20}$  such a state is, for example, given by

$$(2s_{1/2})^{-1}(1f_{7/2}).$$

The Fermi level coincides in this case with the  $1d_{3/2}$  level (see Fig. 2.5).

If we use the indices  $i, j$  for the levels below the Fermi surface ( $\epsilon_i < \epsilon_F$ ), and the indices  $m, n$  for the levels above the Fermi surface ( $\epsilon_n > \epsilon_F$ ), the lowest excitations in the shell model are then  $ph$  excitations of the form

$$|\Phi_{mi}\rangle := a_m^+ a_i |\Phi_0\rangle = \pm a_m^+ a_1^+ \dots a_{i-1}^+ a_{i+1}^+ \dots a_A^+ |-\rangle \quad (2.28)$$

with excitation energy  $\epsilon_{mi} = \epsilon_m - \epsilon_i$ .

In fact one has observed such states in magic nuclei. They are, however, not the lowest states. As we have already seen in Chapter 1, there are low-lying collective states which cannot be explained in the independent particle model.

The Slater determinants (2.23) form a *complete set* of states for the  $A$  nucleon system [Lö 55]. Each state of the system is characterized by the distribution of the nucleons among the levels of the single particle potential, that is, by the "occupation numbers" of the levels. It is usual to classify all excited states by taking the ground state as a reference state. The nucleons that are missing in the ground state are denoted by holes, those above the Fermi levels by particles. A typical multiparticle-multiphole configuration is shown in Fig. 2.8

Starting from a magic nucleus with the mass number  $A$ , we can add a particle and obtain a nucleus with the mass number  $A+1$ . If we put the

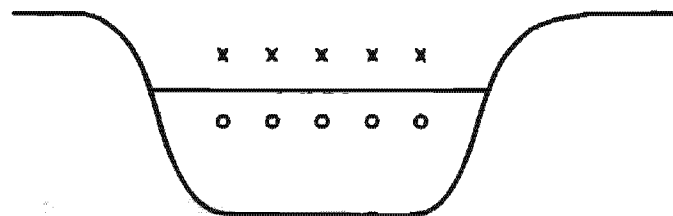


Figure 2.8. Schematic representation of a typical five-particle (crosses), five-hole (open circles) state.

particle into the level  $m$ , the wavefunction is

$$|\Phi_m\rangle = a_m^+ |\Phi_0\rangle \quad (2.29)$$

and we get the energy difference

$$\epsilon_m = E_m(A+1) - E_0(A). \quad (2.30)$$

In this way one is able to measure the single-particle energies (see Sec. 2.7). These are the simplest states in  $A+1$  nuclei. More complicated states have a  $2p-1h$  structure, and so on. In complete analogy, there are  $1h, 1p-2h$ , etc., states in  $A-1$  nuclei.

It often turns out to be very convenient to define quasiparticles by the operators

$$\begin{aligned} \alpha_m^+ &= a_m^+, & \alpha_m &= a_m, & \text{for } \epsilon_m > \epsilon_F; \\ \alpha_i^+ &= a_i, & \alpha_i &= a_i^+, & \text{for } \epsilon_i \leq \epsilon_F. \end{aligned} \quad (2.31)$$

These quasiparticles are again fermions. They are particles for states above, and holes for states below, the Fermi surface, so that we have

$$\alpha_k |\Phi_0\rangle = 0, \quad (2.32)$$

that is, the ground state of the magic nucleus is a "vacuum" with respect to these quasi-particles;  $ph$  states are two-quasi-particle states, and so on. The multi-quasi-particle states

$$|\Phi_{k_1 \dots k_n}\rangle = \alpha_{k_1}^+ \dots \alpha_{k_n}^+ |\Phi_0\rangle \quad (2.33)$$

form a complete orthogonal set in the many-body Hilbert space.

This basis is often used for further investigation of the many-body Hamiltonian  $H$  (2.19). In the shell model, one decomposes  $H$ ,

$$H = T + \sum_{i < j} v(i, j) = H_0 + V_R, \quad (2.34)$$

with the residual interaction

$$V_R = \sum_{i < j} v(i, j) - \sum_i V(i) \quad (2.35)$$

in such a way that  $V_R$  is as small as possible and can be neglected. More elaborate theories investigate  $V_R$  in the basis in which  $H_0$  is diagonal, the shell model basis (see Chap. 8).

The exact ground state wave function of a magic nucleus has the form

$$|\Psi_0\rangle = C_0 |\Phi_0\rangle + \sum_{mi} C_{mi} \alpha_m^+ \alpha_i^+ |\Phi_0\rangle + \frac{1}{4} \sum_{\substack{mi \\ m'i'}} C_{mim'i'} \alpha_m^+ \alpha_m^+ \alpha_i^+ \alpha_{i'}^+ |\Phi_0\rangle + \dots \quad (2.36)$$

If the shell model is a good approximation to the nucleus, the coefficients  $C_{mi}$ ,  $C_{mim'i'}$ , etc. should be small (see Fig. 10.3).

At this point we would like to again stress the fact that we have always been talking about a *spherical shell model* potential. Since, as we shall see, spherical nuclei exist only in the neighborhood of magic nuclei, by the same token this means that we have restricted our discussion to such nuclei. As this spherical average potential is created by the nucleons themselves, it may depend (though not abruptly) on the nucleon number  $A$  in quite a subtle way, in contrast to the atomic case. It is such that we

cannot take a once-and-for-all fixed single-particle potential and hope to find the corresponding single-particle states realized very accurately, be it even over a very limited range of neighboring nuclei.

We should keep these precautions in mind when talking about the shell model. As we said, the filling of the shells is without ambiguity, if we have closed shells. When we start filling neutrons and protons in *unfilled shells* these states will be degenerate, because the  $j$ -shells have a  $(2j+1)$ -fold degeneracy. The configuration of the nucleus can then be characterized by two numbers,  $\kappa$  and  $\lambda$ , which stand for the proton and neutron numbers, respectively, in the partially filled  $j$ -shell. Let the partially filled neutron shell be characterized by the quantum numbers  $(n \ l \ j)$ , and the partially filled proton shell by  $(n' \ l' \ j')$ . One then denotes the configuration by

$$(vnlj)^{\kappa} (\pi n' l' j')^{\lambda}.$$

Because of the  $2j+1$ -fold degeneracy of each  $j$ -shell, all possible shell model states corresponding to this configuration are also degenerate. The number of antisymmetric, linearly independent products is given by the product of the binomial coefficients

$$\binom{2j+1}{\kappa} \binom{2j'+1}{\lambda}. \quad (2.37)$$

The degeneracy of all these states will, of course, be removed in reality due to the action of the residual interaction  $V_R$  (2.35), which is neglected in the shell model. Taking one of the phenomenological nucleon–nucleon forces, as discussed in Chapter 4, one can diagonalize  $V_R$  in the subspace (2.37). Usually one takes not only this subspace into account, but also the one which corresponds to the nearly degenerate levels of a whole major shell. The  $s_{1/2}$ ,  $d_{5/2}$ ,  $d_{3/2}$  levels of the  $s-d$  shell is such a case, covering nuclei from  $^{16}\text{O}$  up to  $^{40}\text{Ca}$ . One can easily be convinced that the dimension of the matrices to be diagonalized becomes exceedingly large for more than two particles in open shells. Special procedures have been developed to diagonalize such huge matrices [Wh 72, SZ 72, WWC 77].

To reduce the size of these matrices, symmetries such as isospin or angular momentum (see Sec. 2.6) can be of great help (see, for instance, [FHM 69, WMH 71, HMW 71, GED 71, VGB 72, Wi 76]).

## 2.6 Symmetry Properties

### 2.6.1 Translational Symmetry

For any solution of the eigenvalue problem (2.19) we must require that a series of symmetry or invariance properties are fulfilled. Among these are, for example, translational and rotational invariance.\* In the shell model

\* Besides these exact symmetries, in some regions of the periodic table one often also has approximate symmetries, as, for instance, the isospin (see Sec. 2.6.3), which can be used for a classification of spectra (see [He 73a]).

one of these invariances is always violated: the *translational invariance*. This comes from the fact that we have to fix the potential in space in contradiction to the homogeneity of space. The most serious consequence of this violation is the appearance of spurious states in the excitation spectrum of the system. This occurs because we have introduced redundant degrees of freedom. If we fix the nucleus in space, it has only  $3A - 3$  spatial degrees of freedom left. The shell model, however, contains  $3A$  variables. These spurious states are therefore not true excitations of the system, but correspond to motions of the nucleus as a whole. Almost all approximation schemes in nuclear physics have inherent symmetry violations. In Chapter 11 we will, therefore, show in fair detail how such violations can be removed.

## 2.6.2 Rotational Symmetry

The spherical shell model Hamiltonian  $H_0$  (ls term included) conserves rotational symmetry. Therefore, it is possible to construct eigenstates of the total angular momentum

$$\mathbf{J} = \sum_{i=1}^A \mathbf{j}^{(i)} \quad \text{and} \quad J_z = \sum_{i=1}^A j_z^{(i)} \quad (2.38)$$

by a linear combination of the Slater determinants (2.23). The closed shell ground state is not degenerate; the only nondegenerate angular momentum eigenstate has  $I=0$ , which is therefore identified with the ground state. This consequence is experimentally confirmed with no exception. It is then clear that, having only one nucleon outside closed shells, the ground state angular momentum of such even-odd nuclei will correspond to the  $j$ -value of the odd nucleon. The same, of course, is true if there is one nucleon missing (a hole) in a filled shell. This rule is also experimentally confirmed with only very few exceptions.

If we fill (remove) more than one particle into (from) an unfilled (filled)  $j$ -level, the situation gets more complicated, because different  $I$ -values will be degenerate. Again, we can remove this degeneracy by diagonalizing the residual interaction. The matrices are now much smaller as we get one for each  $I$  value.

The construction of eigenfunctions of  $\mathbf{J}^2$  will be shown explicitly for a very simple example (for more complicated situations, see [ST 63]). Suppose that in a  $j$ -shell there are only two protons, the configuration of which is then  $(\pi)^2$ . Out of the degenerate two-particle states (which we want to denote by  $|m_1 m_2\rangle$ ,  $m$  being the magnetic quantum number), we construct, according to the rules of angular momentum coupling, an eigenstate  $|IM\rangle$  of  $\mathbf{J}^2$  and  $J_z$  with

$$\mathbf{J}^2 = (\mathbf{J}_1 + \mathbf{J}_2)^2. \quad (2.39)$$

We obtain

$$|IM\rangle = \frac{1}{\sqrt{2}} \sum_{m_1 m_2} C_{m_1 m_2}^J |m_1 m_2\rangle. \quad (2.40)$$



Using the symmetry properties of the Clebsch-Gordan coefficients, (see [Ed 57, Eq. (3.5.14)]), we have with proper normalization

$$|IM\rangle = \frac{1}{\sqrt{8}} \sum_{m_1 m_2} (C_{m_1 m_2}^{j j I M} + (-)^{2j-I} C_{m_2 m_1}^{j j I M}) |m_1 m_2\rangle \quad (2.41)$$

which, upon noting the antisymmetry  $|m_2 m_1\rangle = -|m_1 m_2\rangle$  yields

$$|IM\rangle = \frac{1}{\sqrt{8}} \sum_{m_1 m_2} C_{m_1 m_2}^{j j I M} (1 + (-)^{2j-I+1}) |m_1 m_2\rangle. \quad (2.42)$$

We see from Eq. (2.42) that  $|IM\rangle$  is only different from zero for

$$2j - I + 1 = 2n \quad \text{or} \quad I = 2n; \quad n = 0, 1, 2, \dots, \quad (2.43)$$

that is, for even angular momenta. Taking as a definite example  $j = 3/2$ , we see that the six independent components

$$|m_1 m_2\rangle : |\frac{3}{2} \frac{1}{2}\rangle, |\frac{3}{2} - \frac{1}{2}\rangle, |\frac{3}{2} - \frac{3}{2}\rangle, |\frac{1}{2} - \frac{1}{2}\rangle, |\frac{1}{2} - \frac{3}{2}\rangle, |-\frac{1}{2} - \frac{3}{2}\rangle$$

have been transformed by a unitary transformation to the six angular momentum coupled components, which are degenerate among themselves:

$$|IM\rangle : |00\rangle, |22\rangle, |21\rangle, |20\rangle, |2-1\rangle, |2-2\rangle.$$

In the general case these considerations are a little tedious. In Table 2.1 the possible total angular momenta for a pure proton configuration are presented.

The factor  $1/\sqrt{2}$  in Eq. (2.40) is a normalization in the case in which both particles are in the same shell. In general, we have for the coupling of two particles:

$$(a_{nj}^+ a_{n'j'})_{JM} = \frac{1}{\sqrt{1 + \delta_{jj'} \delta_{nn'}}} \sum_{mm'} C_{m m'}^{j j' I M} a_{njm}^+ a_{n'j'm'}. \quad (2.44)$$

Special care has to be applied in coupling hole states. The operator  $a_{njm}^+$  transforms like the eigenfunction  $\phi_{njm}$ , that is cogredient, under a rotation of the coordinate system and therefore like a spherical tensor of rank  $j$  (i.e., with  $D_{mm'}^j$ ; see Appendix A). On the other hand, the annihilation operator  $a_{njm}$  transforms with  $D_{mm'}^{j*}$ , that is, contragredient. The normal coupling rules (2.44) apply only for tensors, which are both cogredient or both contragredient. We can therefore only couple  $a_{njm}^+$  with the time reversed operator (see [Me 61]),

$$a_{njm}^- = T a_{njm} T^+ = (-)^{j-m} a_{nj, -m}, \quad (2.45)$$

which is, of course, cogredient. The  $ph$  coupling rule is therefore

$$(a_{nj}^+ a_{n'j'})_{JM} = \sum_{mm'} (-)^{j'-m'} C_{m m'}^{j j' I M} a_{njm}^+ a_{n'j', -m'}, \quad (2.46)$$

where we have left out the unimportant phase  $(-)^{j'+1}$ .

From pure angular momentum coupling one cannot as yet decide which of the degenerate states corresponds to the ground state. For that we have, as we have said, to diagonalize  $V_R$  in a certain subspace. This confirms, in general, the experimentally observed rule that even-even groundstates have  $I = 0$ .

Another experimentally found coupling rule which the pure shell model cannot explain without configuration mixing is the fact that even odd nuclei far from closed shells have ground state spins equal to the  $j$ -value of the odd particle. We will see in Chapter 6 how this finds a natural explanation by taking correlations of the nucleons into account.

**Table 2.1** List of possible total angular momenta  $I$  for the configuration  $(j)^n$  ([MJ 55, p. 64])

$n$	
$j = \frac{1}{2}$	1 $\frac{1}{2}$
$j = \frac{3}{2}$	1 $\frac{3}{2}$ 2 0, 2
$j = \frac{5}{2}$	1 $\frac{5}{2}$ 2 0, 2, 4 3 $\frac{3}{2}, \frac{5}{2}, \frac{7}{2}$
$j = \frac{7}{2}$	1 $\frac{7}{2}$ 2 0, 2, 4, 6 3 $\frac{3}{2}, \frac{5}{2}, \frac{7}{2}, \frac{9}{2}, \frac{11}{2}, \frac{13}{2}$ 4 0, 2 (twice), 4 (twice), 5, 6, 8
$j = \frac{9}{2}$	1 $\frac{9}{2}$ 2 0, 2, 4, 6, 8 3 $\frac{3}{2}, \frac{5}{2}, \frac{7}{2}, \frac{9}{2}$ (twice), $\frac{11}{2}, \frac{13}{2}, \frac{15}{2}, \frac{17}{2}$ 4 0 (twice), 2 (twice), 3, 4 (3 times), 5, 6 (3 times), 7, 8 (twice), 9, 10, 12 5 $\frac{1}{2}, \frac{3}{2}, \frac{5}{2}$ (twice), $\frac{7}{2}$ (twice), $\frac{9}{2}$ (3 times), $\frac{11}{2}$ (twice), $\frac{13}{2}$ (twice), $\frac{15}{2}$ (twice), $\frac{17}{2}$ (twice), $\frac{19}{2}, \frac{21}{2}, \frac{23}{2}$
$j = \frac{11}{2}$	1 $\frac{11}{2}$ 2 0, 2, 4, 6, 8, 10 3 $\frac{3}{2}, \frac{5}{2}, \frac{7}{2}, \frac{9}{2}$ (twice), $\frac{11}{2}$ (twice), $\frac{13}{2}, \frac{15}{2}$ (twice), $\frac{17}{2}, \frac{19}{2}, \frac{21}{2}, \frac{23}{2}, \frac{25}{2}$ 4 0 (twice), 2 (3 times), 3, 4 (4 times), 5 (twice), 6 (4 times), 8 (4 times), 9 (twice), 10 (3 times), 11, 12 (twice), 13, 14, 16 5 $\frac{1}{2}, \frac{3}{2}$ (twice), $\frac{5}{2}$ (3 times), $\frac{7}{2}$ (4 times), $\frac{9}{2}$ (4 times), $\frac{11}{2}$ (5 times), $\frac{13}{2}$ (4 times), $\frac{15}{2}$ (5 times), $\frac{17}{2}$ (4 times), $\frac{19}{2}$ (4 times), $\frac{21}{2}$ (3 times), $\frac{23}{2}$ (3 times), $\frac{25}{2}$ (twice), $\frac{27}{2}$ (twice), $\frac{29}{2}, \frac{31}{2}, \frac{33}{2}$ 6 0 (3 times), 2 (4 times), 3 (3 times), 4 (6 times), 5 (3 times), 6 (7 times), 7 (4 times), 8 (6 times), 9 (4 times), 10 (5 times), 11 (twice), 12 (4 times), 13 (twice), 14 (twice), 15, 16, 18

### 2.6.3 The Isotopic Spin

Up to now we have always considered the neutrons and protons separately. As a consequence we have, for example, in Eq. (2.23), a product of two Slater determinants—one for protons and one for neutrons. Apart from their electromagnetic interactions, protons and neutrons have practically the same physical properties. We will see, for instance, in Chapter 4, that nuclear forces are to a large extent independent of whether we consider protons or neutrons—that is, they are charge independent. As long as the influence of the Coulomb force on the nuclear properties can be neglected, we can consider the proton and the neutron as just two